Evaluating hydroclimatic change signals from statistically and dynamically downscaled GCMs and hydrologic models

Rajesh R. Shrestha, Markus A. Schnorbus, Arelia T. Werner, and Francis W. Zwiers

2014

Pacific Climate Impacts Consortium (PCIC)

PCIC Publications

Original citation:
Shrestha, R. R., Schnorbus, M. A., Werner, A. T., & Zwiers, F. W. (2014). Evaluating hydroclimatic change signals from statistically and dynamically downscaled GCMs and hydrologic models. *Journal of Hydrometeorology, 15*(2), 844-860. https://doi.org/10.1175/JHM-D-13-030.1

Evaluating Hydroclimatic Change Signals from Statistically and Dynamically Downscaled GCMs and Hydrologic Models

RAJESH R. SHRESTHA, MARKUS A. SCHNORBUS, ARELIA T. WERNER, AND FRANCIS W. ZWIERS

Pacific Climate Impacts Consortium, University of Victoria, Victoria, British Columbia, Canada

(Manuscript received 14 February 2013, in final form 3 October 2013)

ABSTRACT

This study analyzed potential hydroclimatic change in the Peace River basin in the province of British Columbia, Canada, based on two structurally different approaches: (i) statistically downscaled global climate models (GCMs) using the bias-corrected spatial disaggregation (BCSD) and (ii) dynamically downscaled GCM with the Canadian Regional Climate Model (CRCM). Additionally, simulated hydrologic changes from the GCM–BCSD-driven Variable Infiltration Capacity (VIC) model were compared to the CRCM integrated Canadian Land Surface Scheme (CLASS) output. The results show good agreements of the GCM–BCSD–VIC simulated precipitation, temperature, and runoff with observations, while the CRCM-simulated results differ substantially from observations. Nevertheless, differences (between the 2050s and 1970s) obtained from the two approaches are qualitatively similar for precipitation and temperature, although they are substantially different for snow water equivalent and runoff. The results obtained from the five Coupled Global Climate Model, version 3, (CGCM3)-driven CRCM runs are similar, suggesting that the multidecadal internal variability is not a large source of uncertainty for the Peace River basin. Overall, the GCM–BCSD–VIC approach, for now, remains the preferred approach for projecting basin-scale future hydrologic changes, provided that it explicitly accounts for the biases and includes plausible snow and runoff parameterizations. However, even with the GCM–BCSD–VIC approach, projections differ considerably depending on which of an ensemble of eight GCMs is used. Such differences reemphasize the uncertain nature of future hydroclimatic projections.

1. Introduction

Global climate models (GCMs) are the primary tools for projecting climate. However, direct GCM output is difficult to interpret from a basin-scale hydroclimatic perspective owing to the limited resolution and lack of sufficiently detailed representation of land surface processes at the basin scale. Thus, at a basin scale, it is customary to employ a downscaling technique for a finer spatial-scale representation of the climatic variables. Statistical or empirical downscaling techniques that relate the GCM output to the local climate have been widely used for this purpose, such as bias-corrected spatial disaggregation (BCSD) (Wood et al. 2002), TreeGen (Stahl et al. 2008), and constructed analog (Maurer and Hidalgo 2008). For hydrologic impact studies, a commonly used approach (hereafter referred to as approach 1) is to statistically downscale GCM outputs to drive a hydrologic model, which is set up and calibrated at a basin scale (e.g., Wood et al. 2004; Hidalgo et al. 2009; Allen et al. 2010).

Dynamical downscaling, in which a GCM provides boundary conditions for a regional climate model (RCM), provides an alternate pathway for projecting future hydroclimatic conditions. The RCMs offer finer spatial resolution (typically 25–50-km resolution) than the GCMs, allowing for greater topographic complexity and finer-scale atmospheric variability to be simulated, and arguably representing a more adequate tool for generating information required for regional impact studies (Sushama et al. 2006). Compared to statistical downscaling, the main advantage of using RCMs is their ability to respond in a physically and spatially consistent way to different external forcings such as land surface or atmospheric chemistry change (Wilby et al. 2000) and to maintain dynamic balances across a range of climate variables. Nevertheless, RCMs have biases and deficiencies of their own (e.g., Plummer et al. 2006). Recent improvements in RCMs include the integration of sophisticated land surface schemes to provide lower boundary conditions for the atmosphere and handling

Corresponding author address: Dr. Rajesh R. Shrestha, Pacific Climate Impacts Consortium, University House 1, P.O. Box 3060, Stn. CSC, University of Victoria, Victoria, BC V8W 3R4, Canada. E-mail: rshresth@uvic.ca

DOI: 10.1175/JHM-D-13-030.1

surface energy and moisture fluxes. Such advances have led to the use of RCMs, such as the Canadian Regional Climate Model (CRCM) (Sushama et al. 2006; Poitras et al. 2011), the Regional Climate Model (RegCM) (Winter and Eltahir 2011a,b), and the Weather Research and Forecasting Model (WRF) (Salathé et al. 2010) without further downscaling, for regional- and basin-scale hydroclimatic diagnostics. These studies demonstrated the effectiveness of RCMs in capturing hydroclimatic change signals, such as increased evaporative demand (Winter and Eltahir 2011b), reduced snowpack (Salathé et al. 2010), increased winter streamflow, and earlier snowmelt-driven peak flow (Sushama et al. 2006; Poitras et al. 2011). Such projected changes are similar to the projections using the approach 1 (Merritt et al. 2006; Rauscher et al. 2008; Elsner et al. 2010; Vano et al. 2010; Shrestha et al. 2012a,b). Given such advances, and the availability of multiple RCMs [e.g., the North American Regional Climate Change Assessment Program (NARCCAP) (Mearns et al. 2009) and the Coordinated Regional Climate Downscaling Experiment (CORDEX) (Giorgi et al. 2009)], the use of the RCM-based approach (hereafter referred to as approach 2) for evaluating future hydroclimatic changes can be expected to become more popular.

However, the ability of the RCMs to simulate hydroclimatic changes is not entirely clear, especially given that the RCMs are typically biased (e.g., Plummer et al. 2006; Sushama et al. 2006; Rivington et al. 2008; Teutschbein and Seibert 2012; Muerth et al. 2013). The biases arise from both the driving GCM and RCM structure, and the driving GCM biases may be reduced or amplified by the RCM (Gao et al. 2011). The effect of biases in the driving variables (e.g., precipitation and temperature) on hydrologic variables (e.g., runoff and snow) is also not fully understood. In contrast, statistical downscaling methods, such as BCSD, correct the biases in a given GCM for the current climate by comparing GCM values with observations and assuming that biases for the future climate are equivalent to the current climate. Furthermore, the two approaches differ significantly in model structure, resolution, and scale. Specifically, while the hydrologic models are set up at a watershed or river basin scale with a detailed representation of topography, land cover, and soil (typically at a resolution of 100 m to 5 km), the RCMs are set up for a larger domain (typically continental or subcontinental scale) and discretized at a coarser resolution (typically 25–50 km resolution). The effect of model resolution can be critical in mountainous regions, such as the physiographically heterogeneous and hydroclimatologically complex Pacific Northwest region. Given the large domain size and atmosphere–land surface process integration, multiple RCM runs are computationally expensive, and, in general, only a limited number of ensemble members are available. However, for end users, RCM outputs are easy to extract and analyze for hydroclimatic assessments. In contrast, hydrologic models generally require limited computational time; therefore, they can be used efficiently to run large ensembles of climate scenarios. Another major difference is in the parameterization of the two models. While a hydrologic model is typically parameterized by calibrating with observed streamflow, the RCM land surface parameters are not normally tuned to match observed streamflow from a catchment.

The results obtained from the two approaches also need to be considered in the context of associated uncertainties. Kay et al. (2008) outlined different sources of uncertainties in the assessment of hydrologic impacts of climate change, which include future greenhouse gas emissions (forcings), GCM/RCM structure, downscaling method, hydrologic model structure, hydrologic model parameters, and natural variability of the climate system. In particular, studies using approach 1 with ensembles of GCMs (e.g., Kay et al. 2008; Prudhomme and Davies 2008a,b; Najafi et al. 2011; Bennett et al. 2012) indicate that GCM structure (i.e., differences due to the physical processes as represented by different GCMs) is the largest source of uncertainty in projected hydrologic impacts. The climate's natural chaotic internal variability, which is also simulated by climate models, could also have appreciable impacts on the sensitivity of some of the outputs (e.g., Lucas-Picher et al. 2008; Kendon et al. 2010; Deser et al. 2012).

Given the differences and uncertainties in these two structurally different approaches, an important question arises concerning the confidence that we can have in the model-simulated hydroclimatic changes. This paper attempts to fill this gap in our understanding. The novelty of this paper is to provide insights on climate change signals in light of propagated biases and uncertainties and to provide an assessment of the general suitability of using the two approaches for future hydroclimatic projections. Precipitation and temperature outputs from the statistical downscaling (using BCSD) (approach 1) and dynamical downscaling (with CRCM) (approach 2) were compared. Simulated hydrologic response (to the meteorological inputs) from the GCM–BCSD-driven Variable Infiltration Capacity (VIC) model (Liang et al. 1994, 1996) were compared to the CRCM integrated Canadian Land Surface Scheme (CLASS) (Verseghy 1991; Verseghy et al. 1993; Verseghy 2000) output. An evaluation of the sensitivities of the external forcings for the two approaches was undertaken by using an ensemble of eight GCMs and five CRCM runs, respectively.

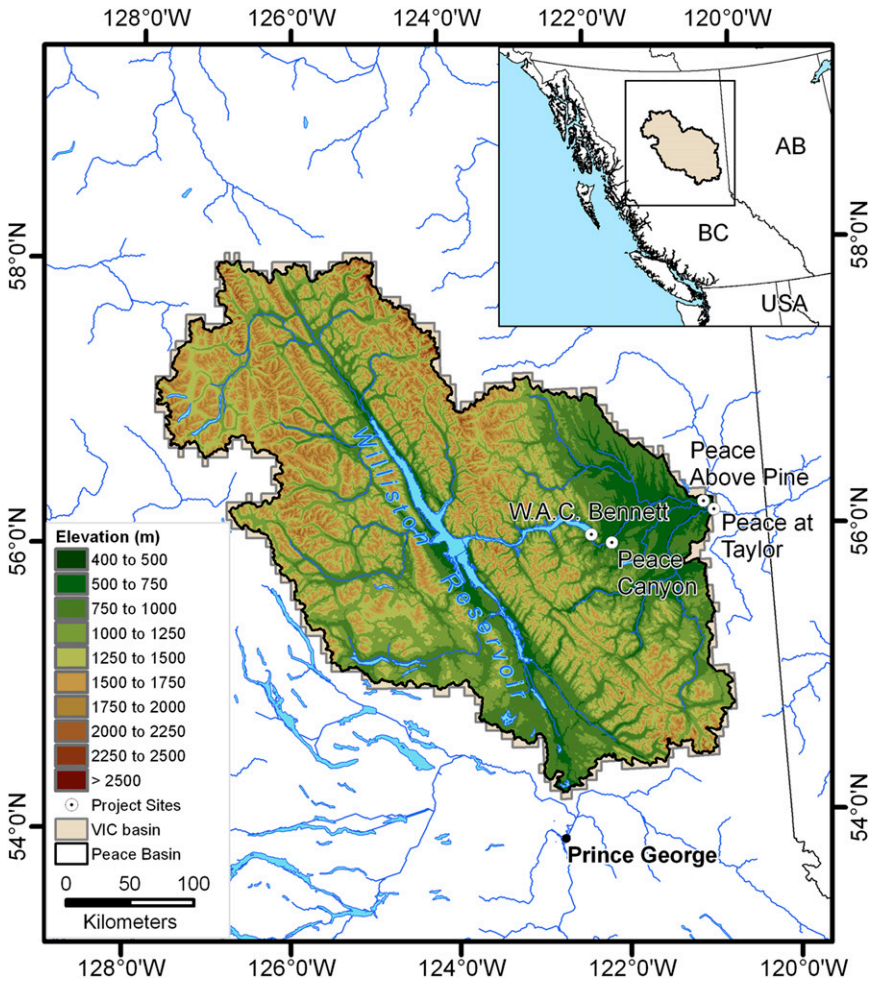

FIG. 1. Location map and elevation range of the Peace River basin.

2. Study basin and data

The Peace River basin study area covers a drainage area of approximately 101 000 km^2 upstream of Taylor in interior northeastern British Columbia (BC), Canada (Fig. 1). The river has its headwaters in the northern Rocky Mountains and relief ranges from 400 to about 2900 m (Fig. 1). The Peace River and its tributaries flow through diverse physiographic regions, including the Central Canadian Rocky Mountains and the Alberta Plateau ecoregions (Demarchi 2011), and discharge into the inland Peace–Athabasca delta and ultimately into Great Slave Lake.

The Peace River basin has a cold continental climate, which is typical for northern North America. Mean annual precipitation is about 810 mm, with a slightly higher seasonal amount in the summer (31% of the annual accumulation) and lower amount in the winter (17%) (based on gridded data primarily derived from the Environment Canada climate station observations). Approximately 54% of annual precipitation falls as snow, mostly during October through April (based on the VIC model partitioning of the gridded precipitation data). The mean annual cycle of air temperature (monthly means) varies between −12° and +12°C, with the basin remaining below freezing from December to March. The Peace River is regulated for hydroelectric power by the W. A. C. Bennett Dam that forms the Williston Lake Reservoir and the Peace Canyon Dam that forms the Dinosaur Reservoir System (Fig. 1). This study does not consider regulated flow from the reservoir system but instead uses naturalized flow for the hydrologic model calibration. The naturalized flow from each reservoir is estimated based on outflow and the reservoir level, which is routed together with flows from unregulated tributaries to a downstream station (BC Hydro 2004, unpublished data). The use of the naturalized flow contributes to uncertainty in the observed runoff used in this study. However, since the comparisons are made at a monthly time step, error in estimating the naturalized

flow (such as daily flow) is not considered to be critical. The mean annual naturalized streamflow (1968–90) of the Peace River at the Taylor hydrometric station (at the Water Survey of Canada hydrometric station 07FD002) is about 1400 $m^3 s^{-1}$, with the maximum and minimum monthly mean flows in June (~4700 $m^3 s^{-1}$) and February (~300 $m^3 s^{-1}$), respectively. The Peace River basin has a snowmelt-driven hydrologic regime in which about 65% of the annual flow occurs between May and July. The glaciated area in the Peace River basin is very small (~0.4%) and is not considered in this study.

3. Methods

a. *Statistical downscaling of GCMs and hydrologic modeling*

In approach 1, daily gridded observations (spatial resolution of 1/16°) were used for calibrating/validating the VIC model and simulating baseline hydrologic conditions. Gridded maximum and minimum temperature and precipitation data were generated for the entire province of British Columbia primarily from the Environment Canada climate station observations, with supplementary inputs from the U.S. Cooperative Station Network, the British Columbia Ministry of Forests and Range's Fire and Weather Network, the British Columbia Ministry of Environment's Automated Snow Pillow (ASP) network, and the BC Hydro climate network (see Schnorbus et al. 2011). Daily average wind speed is based on estimates of 10-m wind speed from the National Centers for Environmental Prediction–National Center for Atmospheric Research (NCEP–NCAR) reanalysis (Kalnay et al. 1996).

BCSD (Wood et al. 2004) was employed to statistically downscale the coarse-resolution GCM outputs. Previous studies (e.g., Maurer and Hidalgo 2008; Bürger et al. 2012) have demonstrated the effectiveness of BCSD in capturing many aspects of historical daily variability, including temperature extremes, and found the method to be competitive in this respect with many other statistical downscaling methods. BCSD performs downscaling in three steps: (i) bias correction of the large-scale monthly GCM fields against aggregated gridded observations using quantile mapping (rescaled based on mean and variance), (ii) spatial disaggregation of the bias-corrected monthly fields to a finer resolution (to match the resolution of the VIC model) using a ''local scaling'' approach, and (iii) temporal disaggregation of the locally scaled monthly fields to the daily historic records. The BCSD was calibrated with the observed precipitation and minimum and maximum air temperature for the period 1950–90 and validated for the period 1991–2000. Future wind data were created based on the historical wind data as represented in the NCEP–NCAR reanalysis (Kalnay et al. 1996). First analog months were selected based on having sufficient precipitation volumes to support the amount of precipitation in the future GCM (Werner 2011). Temperature and wind were then taken from the same precipitation day, with the temperature scaled so that the monthly value matches those of the GCM being downscaled, while the winds were taken as is from the NCEP–NCAR reanalysis. Hence, future wind speed was not downscaled from the GCMs. A detailed description of the GCM selection, BCSD, and gridded data generation for hydroclimate projections over BC is available in Werner (2011).

The spatially distributed macroscale VIC hydrologic model version 4.0.7 (Liang et al. 1994, 1996) was employed in a water balance mode for the Peace River basin. VIC computes water fluxes for a range of hydrologic processes such as evapotranspiration, snow accumulation, snowmelt, infiltration, soil moisture, and surface and subsurface runoff. The model represents soil moisture processes in three soil layers and represents subgrid variability of land surface vegetation classes and topography by partitioning each grid cell into a number of mosaic-type land cover tiles and elevation (snow) bands, respectively. Simulated fluxes as well as state variables for each grid cell are calculated as area averages of subgrid values. VIC explicitly accounts for snow accumulation and ablation by using a two-layer snowpack model individually for each land cover/elevation tile. The model uses variable infiltration curves for runoff generation and the Arno conceptual model (Todini 1996) for subsurface flow generation. Surface runoff from the upper two soil layers is generated when the moisture exceeds the storage capacity of the soil. A detailed description of the VIC model is available in Liang et al. (1994, 1996, 2003).

The VIC model was set up at a $^1/_{16}°$ spatial resolution and daily temporal resolution. Geospatial data for the VIC model were derived from (i) a 90-m resolution digital elevation model from the National Aeronautics and Space Administration Shuttle Radar Topographic Mission (SRTM) (Jarvis et al. 2008), (ii) a 25-m resolution land cover dataset from the Earth Observation for Sustainable Development of Forests (Wulder et al. 2003), and (iii) a $^1/_{12}°$-resolution soil classification and parameterization dataset based on the Soils Program in the Global Soil Data Products CD-ROM (Global Soil Data Task 2000). The VIC model for the Peace River basin was divided into 23 subbasins (based on Water Survey of Canada hydrometric station locations), and streamflow in each subbasin was calibrated by varying six runoff generation parameters. Additionally, fresh

snowpack albedo and its decay rate during snowmelt were adjusted to replicate a slower snowmelt response in the BC river basins (Schnorbus et al. 2010, 2014). A comparison of the 1 April snow water equivalent (SWE) data from 21 snow course sites in the Peace River basin and corresponding model grid boxes showed that the VIC-modeled SWE generally captured the magnitude of observed SWE (Schnorbus et al. 2014). The downscaled GCM outputs (1950–2098), consisting of daily precipitation and minimum and maximum air temperature, were used as inputs to the calibrated VIC model for the simulation of the baseline and future climates. For a detailed description of the VIC model setup, calibration, and climate change projections for the Peace River basin, readers are referred to Schnorbus et al. (2011) and Schnorbus et al. (2014).

b. *Regional climate model and land surface scheme*

In approach 2, hydroclimatic variables for the Peace River basin were extracted from CRCM version 4.2.3 (Music and Caya 2009). The CRCM covers the North American domain at a 45-km grid resolution (true at 60°N on a polar stereographic projection). It is driven at the boundary by the Canadian Global Climate Model version 3 (CGCM3, T47 L32) (Scinocca et al. 2008), and the future climate (2041–70) projection corresponds to the Special Report on Emissions Scenarios (SRES) A2 emissions scenario, which is the emissions scenario used in the NARCCAP (Mearns et al. 2009). Future hydroclimatic projections for 2041–70 are not highly sensitive to the choice of the SRES emission scenarios for BC watersheds (Schnorbus et al. 2014).

The CRCM version 4.2.3 includes the CLASS version 2.7 (Verseghy 2000; Bartlett et al. 2006), which describes the water and energy exchange between the atmosphere and land surface. CLASS comprises three soil layers, a variable-depth snow layer, and a separate vegetation canopy. The subgrid-scale variability in the CLASS model is represented by dividing each grid cell into vegetated and bare soil areas, which are further subdivided into snow-covered and snow-free fractions as necessary (Bartlett et al. 2006). The model considers energy and water fluxes for each soil layer and calculates energy fluxes at the top and bottom of the snowpack (Verseghy 2000). Snowmelt occurs when surface temperature (calculated from the surface energy budget equation) exceeds 0°C (Music and Caya 2007). If the temperature of snow layer falls below 0°C, the water generated by snowmelt or rainwater (in case it rains) refreezes. CLASS uses Darcy's equation (Maidment 1993) to evaluate water fluxes between the layers. When the infiltration capacity is exceeded, water is considered ponded at the surface up to a maximum surface retention

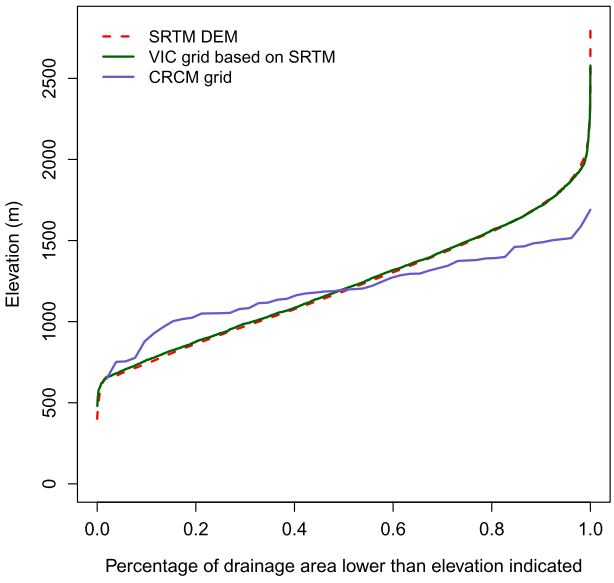

FIG. 2. Hypsometry plots using SRTM DEM (~90-m resolution), VIC grid (~5.5 km) with elevation bands aggregated from the SRTM, and CRCM grid (~45 km) for the Peace River basin.

capacity, beyond which surface runoff occurs. Subsurface flow is calculated from the deepest soil layer as a function of saturated hydraulic conductivity and volumetric liquid water content. More details on the CLASS model are available in Verseghy (1991, 2000) and Verseghy et al. (1993) and its implementation in the CRCM is summarized in Music and Caya (2007, 2009). Evaluation of the CRCM outputs for the study basin is described in detail in Rodenhuis et al. (2011) and Music et al. (2012).

Unlike VIC, CLASS is not explicitly calibrated to local basin streamflow. Nevertheless, some level of parameter tuning is involved; for example, field measurements from specific locations are used to constrain the empirical relationships for hydrologic properties (as a function of texture) or snow thermal conductivity (as a function of density) (Sulis et al. 2011).

c. *Comparison of the two approaches*

The two approaches employed in this study have considerable differences, which include model resolution, model scale, hypsometry (Fig. 2), driving GCMs, downscaling, bias correction, and hydrologic model structure and parameterization (Table 1). In particular, differences due to model resolution could be considerable as it affects the spatial discretization of land cover, soil and hypsometry, and elevation and orographic effects on precipitation. The hydroclimatic change signals from such structurally different approaches was evaluated using the experimental setup summarized in Fig. 3.

TABLE 1. Comparison of model structure and inputs for the two approaches used in this study.

	Approach 1	Approach 2
Resolution	Downscaling of GCM outputs and hydrologic modeling at $^1/_{16}^\circ$ (approximately ~5.5 km^2, depending on latitude/longitude)	CRCM 4.3.2 grid of 45-km horizontal mesh (true at 60°N on a polar stereographic projection)
Scale	Hydrologic model set up at a basin scale	CRCM set up for the North American domain
Hypsometry	Representative hypsometry of the basin (Fig. 2) by $^1/_{16}^\circ$ grids with 500-m interval elevation bands (compared to 90-m SRTM DEM; Jarvis et al. 2008)	Very approximate hypsometry of the basins (Fig. 2) by CRCM grids (compared to 90-m SRTM DEM)
Hydrologic model structure	Hydrologic simulation using a basin-scale hydrologic model (VIC 4.07)	Hydrologic simulation extracted from the CRCM (which includes the CLASS 2.7 model for water and energy exchange between the atmosphere and land surface)
Hydrologic parameterization	The VIC hydrologic model divided into 23 subbasins and the model parameters calibrated with the subbasin streamflows	Parameters of the CLASS model not calibrated to reproduce local streamflow
Climate inputs	CGCM3 run 4 (for GBVS) and a set of eight different GCM runs (for GBVM; Fig. 3)	CGCM3 run 4 (for GRS) and a set of five CGCM3 runs (for GRM; Fig. 3)
Downscaling method	GCM outputs statistically downscaled to the resolution of the VIC model using the BCSD method	CGCM3 dynamically downscaled with the CRCM
Bias correction	GCM biases removed by the BCSD method (nonparametric quantile-mapping technique)	CGCM3/CRCM outputs used without bias correction

Differences due to the two different downscaling methods and hydrologic models were considered by comparing the CGCM3 (run 4)–driven BCSD–VIC [referred to as the GCM–BCSD–VIC–Single (GBVS)] with the CGCM3 (run 4)–driven CRCM [referred to as the GCM–RCM–Single (GRS)]. Sensitivity of the RCM results to the climate model's internal variability was considered by using an ensemble of five CGCM3-driven CRCM runs, referred to as the GCM–RCM–Multiple (GRM). Additionally, the sensitivity of the GBVS results to the differences in the GCM structure was considered by using an ensemble of eight GCMs participating in phase 3 of the Coupled Model Intercomparison Project (CMIP3) (Meehl et al. 2007) (see Table 2), referred to as the GCM–BCSD–VIC–Multiple (GBVM). The GCMs used in the GBVM experiment correspond to run 1 for all GCMs except for the CGCM3 (run 4).

For these evaluations, the baseline climate was represented by the period 1961–90 (1970s), which corresponds to the climate of the twentieth-century run. Since CRCM results are only available for the A2 emissions scenario, the future climate represented by the A2 emissions scenario for the period 2041–70 (2050s) was used. Average basin precipitation, air temperature, and runoff were compared, which were derived by spatially averaging individual grid values. Since the CRCM does not include a routing routine, runoff from both CRCM and VIC were considered without routing. Naturalized streamflow at the basin outlet was normalized by the basin area and the naturalized runoff was generated to allow comparison with the unrouted model output. It should be noted that the unrouted model runoff lacks the effects of routing delays when compared to the naturalized runoff. However, since the mean travel time for the fast runoff component for the basin is about 9 days (from unit hydrograph analysis) and temporal intercomparisons are made at a monthly time step, the effect of such routing delays is not considered to be critical. The outputs were compared for the median values and ranges, with each of the 30-yr values treated as one sample. Future changes were expressed relative to the median value of the 30-yr baseline simulation of

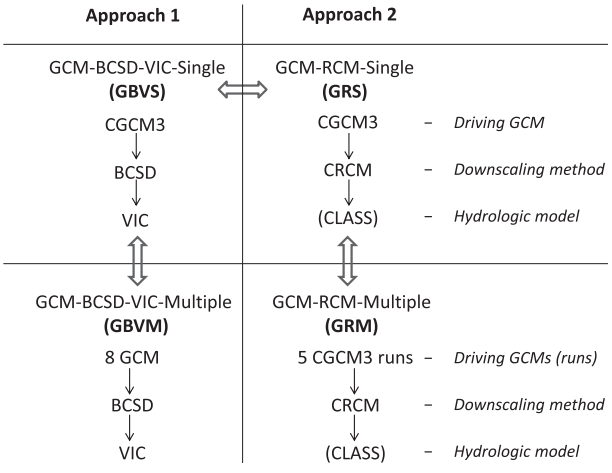

FIG. 3. Summary of the experimental setups using the two approaches. The block arrows show the comparisons performed in this study. The CLASS hydrologic model is integrated into the CRCM and enclosed in parentheses.

TABLE 2. Eight GCMs participating in CMIP3 (Meehl et al. 2007) used in this study.

Model ID	Model	Institution	Atmospheric resolution	Primary reference
CCSM3	Community Climate System Model, version 3	National Center for Atmospheric Research (United States)	T85 L26	Collins et al. (2006)
CGCM3 (T47)	Canadian Centre for Climate Modelling and Analysis (CCCma) Coupled Global Climate Model, version 3	Canadian Centre for Climate Modelling and Analysis (Canada)	T47 L31	Scinocca et al. (2008)
CSIRO Mk3.0	Commonwealth Scientific and Industrial Research Organisation, Mark 3.0	Commonwealth Scientific and Industrial Research Organization (Australia)	T63 L18	Rotstayn et al. (2010)
ECHAM5		Max Planck Institute for Meteorology (Germany)	T63 L32	Roeckner et al. (2006)
GFDL CM2.1	Geophysical Fluid Dynamics Laboratory limate Model, Cversion 2.1	NOAA Geophysical Fluid Dynamics Laboratory (United States)	N45 L24	Delworth et al. (2006)
HadCM3	Hadley Centre Coupled Model, version 3	Hadley Centre for Climate Prediction and Research/Met Office (United Kingdom)	T42 L19	Collins et al. (2001)
HadGEM1	Hadley Centre Global Environment Model, version 1	Hadley Centre for Climate Prediction and Research/Met Office (United Kingdom)	N96 L38	Martin et al. (2006)
MIROC3.2 (medres)	Model for Interdisciplinary Research on Climate, version 3.2	Center for Climate Systems Research (The University of Tokyo), National Institute for Environmental Studies, and Frontier Research Center for Global Change (JAMSTEC) (Japan)	T42 L20	K-1 Model Developers (2004)

the corresponding GCM member or run. Additionally, the two-sided Student's t test with autocorrelation correction (see von Storch and Zwiers 1999) was employed to evaluate whether the mean future changes are different from zero at a 5% significance level. Since pooling together the ensembles (in GRM and GBVM) into one sample to test for statistically significant differences was considered problematic (see von Storch and Zwiers 2013), each member of the ensemble was evaluated separately.

4. Results and discussion

a. Comparison of GBVS and GRS results

We begin with a comparison of monthly precipitation, temperature, evapotranspiration (ET), snow water equivalent (SWE), and runoff derived (Figs. 4a–j) from the two downscaling approaches when using the same driving GCM simulation, CGCM3 run 4 (GBVS and GRS). The red hashed areas show the natural interannual variability as represented by observations for the 30-yr 1961–90 baseline period (Figs. 4a,c,i). Since BCSD was calibrated with the gridded-observed precipitation and temperature data, the 5th, 50th, and 95th percentiles of the observations are closely replicated by the GBVS. The GRS-simulated precipitation has a smaller range, mainly because the range (between 5th and 95th percentiles) has not been scaled to match the distribution of observations (Fig. 4a). The coarser resolution of the CRCM precipitation also implies that there are limitations in resolving elevation and orographic effects. The GRS-simulated precipitation and temperature are biased, with the median precipitation and temperature indicating dry and cold biases, respectively, when compared to the observations (Figs. 4a,c). Specifically, the GRS-simulated precipitation and temperature are drier and colder, respectively, for all seasons (Table 3), with annual precipitation ~18% lower and annual temperature ~6°C colder than observed. Rodenhuis et al. (2011) compared the CRCM results with the driving GCM and observations, which revealed that the precipitation and temperature biases originate predominantly from the driving GCM, and the biases were reduced for precipitation and amplified for temperature by the CRCM. The biases are also reflected in the future period (Figs. 4b,d), with the GRS simulation producing lower median precipitation and temperature values and a narrower precipitation range, compared to the GBVS simulation.

The GBVS and GRS results differ considerably for the ET and SWE results. Specifically, compared to the GBVS results, the GRS-simulated ET values are lower and SWE values are higher (Figs. 4e–h), illustrating the effect of the cold temperature bias. The comparison of the GBVS- and GRS-simulated runoff outputs with normalized observed runoff (Fig. 4i) shows that the GBVS simulates the magnitude and timing of the runoff

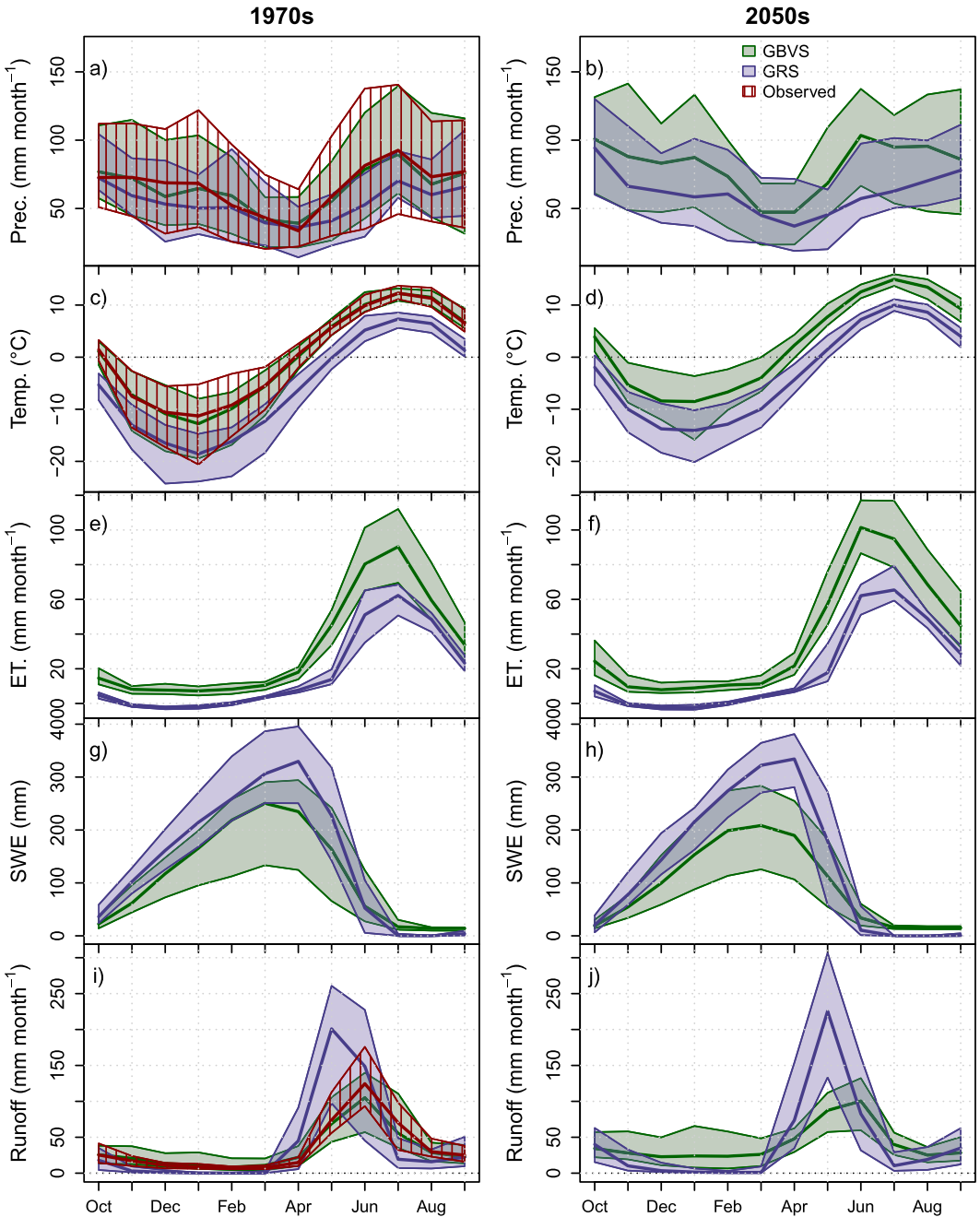

FIG. 4. Comparison of the 1970s and 2050s precipitation, temperature, evapotranspiration (ET), snow water equivalent (SWE), and runoff from the GBVS and GRS. The lower and upper bounds of the ranges show the 5th and 95th percentiles, and the thick lines in the middle show the median values. The observed runoff is based on naturalized flow normalized by the basin area.

peak reasonably well. Such agreement of the VIC-simulated runoff with observations illustrates the efficacy of the bias correction (of driving precipitation and temperature) and calibration (of VIC model parameters). In contrast, the GRS-simulated runoff for the baseline period is noticeably different from the observations and GBVS-simulated runoff. Specifically, the GRS show little or no runoff in winter, while spring runoff is substantially higher than observations (Fig. 4i, Table 3). Additionally, despite lower annual precipitation (~18%), the GRS-simulated annual runoff volume is higher (~14%) than the observed. The runoff ratios

TABLE 3. Comparison of the 30-yr (1961–90) median precipitation and temperature and available 23-yr (1968–90) runoff.

	Winter	Spring	Summer	Autumn	Annual
			Precipitation (mm)		
Observed	189	136	247	222	795
GBVS	183	136	236	225	780
GRS	154	117	183	198	651
			Temperature (°C)		
Observed	−10.4	0.3	11.2	0.1	0.3
GBVS	−11.2	0.2	11.3	0.2	0.1
GRS	−17.1	−6.3	6.3	−5.7	−5.7
			Runoff (mm)		
Observed	28	96	225	68	416
GBVS	33	102	189	69	393
GRS	1	246	184	43	474

(expressed as the ratio of median annual runoff to precipitation) also differ, with the GBVS value (0.50) close to the observed value (0.52) and the GRM value (0.73) higher than observed. Similarly, the runoff ratio for the GRM (0.68) is higher than the GBVS (0.49) for the 2050s. This discrepancy in the GRS can be again attributed to the cold temperature bias, which results in a lower ET (Fig. 4e), higher SWE (Fig. 4g), and consequently higher annual runoff. Furthermore, the magnitude and timing of the April–June runoff peak from the GRS are substantially different from observations and GBVS-simulated results (Fig. 4i), with the GRS results showing earlier snowmelt and peak runoff timing. Such discrepancies cannot be explained by the biases in the driving data (i.e., mean temperature and precipitation biases) since the cold temperature bias in the GRS should cause delayed snowmelt and a delayed runoff peak (when compared to the GBVS simulation). Furthermore, although the CRCM elevations above the median elevations of the region (~1200 m) are lower than in VIC (Fig. 2), snowmelt should still occur later because of the cold bias. Such early snowmelt and runoff peak despite the cold bias was also noted in the previous study of the upper Columbia basin (Shrestha et al. 2011) and in other studies using the CRCM version 4.2 (Gao et al. 2011) and CRCM version 3.5.3 (Langlois et al. 2004). Snowmelt in the CRCM–CLASS is calculated using an energy budget equation (Music and Caya 2007), but a detailed evaluation of different components of the energy budget is beyond the scope of this paper. However, we examined the diurnal temperature cycle in the CRCM and found that, although the mean temperature between March and April remains below 0°C, the maximum temperature changes from −3°C to 3°C (not shown). Such temperature increase could cause partial snowmelt and rainfall and increase in runoff. Additionally, the GRS results also depict a rapid decline of the SWE storage, which could be partly due to CRCM–CLASS parameterizations, such as those for the albedo of fresh snowpack and snowpack metamorphism, which are not locally calibrated. Specifically, fresh snowpack albedo value for the CLASS model (0.84) (Bartlett et al. 2006) is lower than the value used in the VIC model (0.90) (Schnorbus et al. 2010) and remains lower in the CLASS model (compared to the VIC model) with snowmelt (not shown). This would cause faster spring depletion of the snowpack in CLASS and thus faster runoff increase compared to VIC. Furthermore, as illustrated by Davison et al. (2006) and Dornes et al. (2008), calibration of the vegetation, runoff generation, and snow parameters of the CLASS model could potentially improve the snow and surface fluxes.

The biases in the driving precipitation and temperature from the GRS simulations, which have also been documented by the previous RCM-based studies (Sushama et al. 2006; Rivington et al. 2008; Poitras et al. 2011), reinforce the need to account for biases on the CRCM-simulated outputs. A simple method is to express the results in terms of changes (or differences between 2050s and 1980s), provided that the structure of biases between the two periods remains consistent. Figure 5 provides such a comparison for the annual values and shows similarities as well as differences between the GRS and GBVS approaches. Specifically, the range of annual precipitation, temperature, ET, and runoff changes are similar, and changes in means are statistically significant (according to the Student's t test) for the two approaches. Additionally, both precipitation increase (median: 20%) and runoff increase (19%) are higher for the GBVS compared to the GRS (precipitation increase: 15%, runoff increase: 15%), while temperature increases are similar (GBVS: 3.0°C, GRS: 2.9°C). This indicates similar sensitivities of the runoff change to the precipitation change in both approaches. In contrast, the sensitivities of 1 April SWE changes to the precipitation and temperature changes differ in the two approaches, with the median GBVS values depicting a decline, the median GRS depicting essentially no change, and only the GBVS showing a statistically significant change in the mean. Differences in the rainfall–snowfall partitioning in the two approaches probably cause the discrepancy in the SWE values. Specifically, while more winter precipitation in the GBVS is likely to fall as rain (owing to warming), this happens to a lesser extent in the GRS (owing to its lower temperature). The complex relationship of precipitation and temperature with SWE suggests that the use of the simulated SWE changes for the projection of future changes can be problematic when precipitation and temperature are biased.

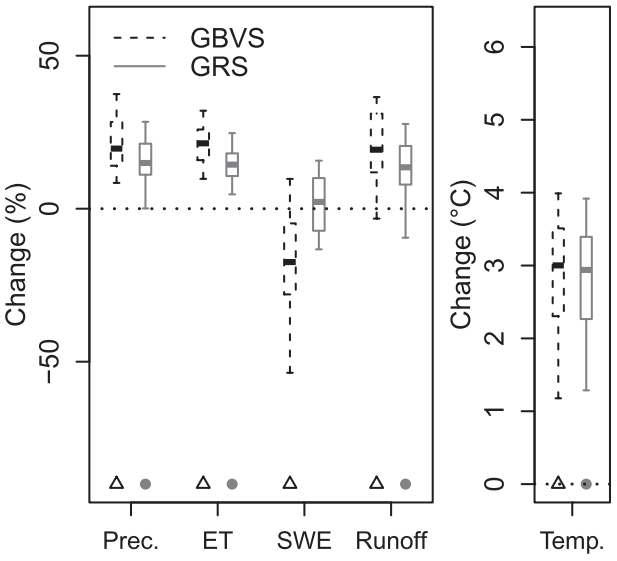

FIG. 5. Annual precipitation, ET, runoff, 1 Apr snow water equivalent (SWE), runoff changes (%), and temperature changes (°C) from the CGCM (run 4)–driven GBVS and GRS. Future changes are expressed relative to median values of the 30-yr baseline simulation. Each box plot illustrates the 25th, 50th, and 75th percentiles, and the whiskers illustrate the 5th and 95th percentiles of the 30-yr period. The triangles and dots at the bottom signify the results with statistically significant changes using the Student's *t* test.

Monthly precipitation, temperature, and runoff changes from the two approaches show large ranges (Fig. 6), owing to the variability of the 30-yr future climate data. Precipitation and temperature changes from the two approaches are mostly consistent (Figs. 6a,b). The results from both approaches depict increased precipitation and temperature, except for the GRS-simulated July precipitation. Projected changes are statistically significant in most months for precipitation and all months for temperature. Since the ranges of 1970s and 2050s GBVS-simulated precipitation are larger (Figs. 4a,b), the range of differences in precipitation is larger when compared to the GRM.

In the case of runoff, the changes are statistically significant for most months and both approaches. Nevertheless, the magnitude of changes from the two approaches differs considerably, especially for December–March and June–August (Fig. 6c). Specifically, the GRS-simulated runoff depicts smaller winter changes (owing to lower temperature) and more pronounced April–May increases and June decreases when compared to the GBVS results. These pronounced changes in the GRS-simulated runoff are related to the rapid decline in the SWE storage. Although a shift to an earlier freshet is also projected by the GBVS, the changes are less pronounced because of smaller winter SWE accumulation and its slower decline

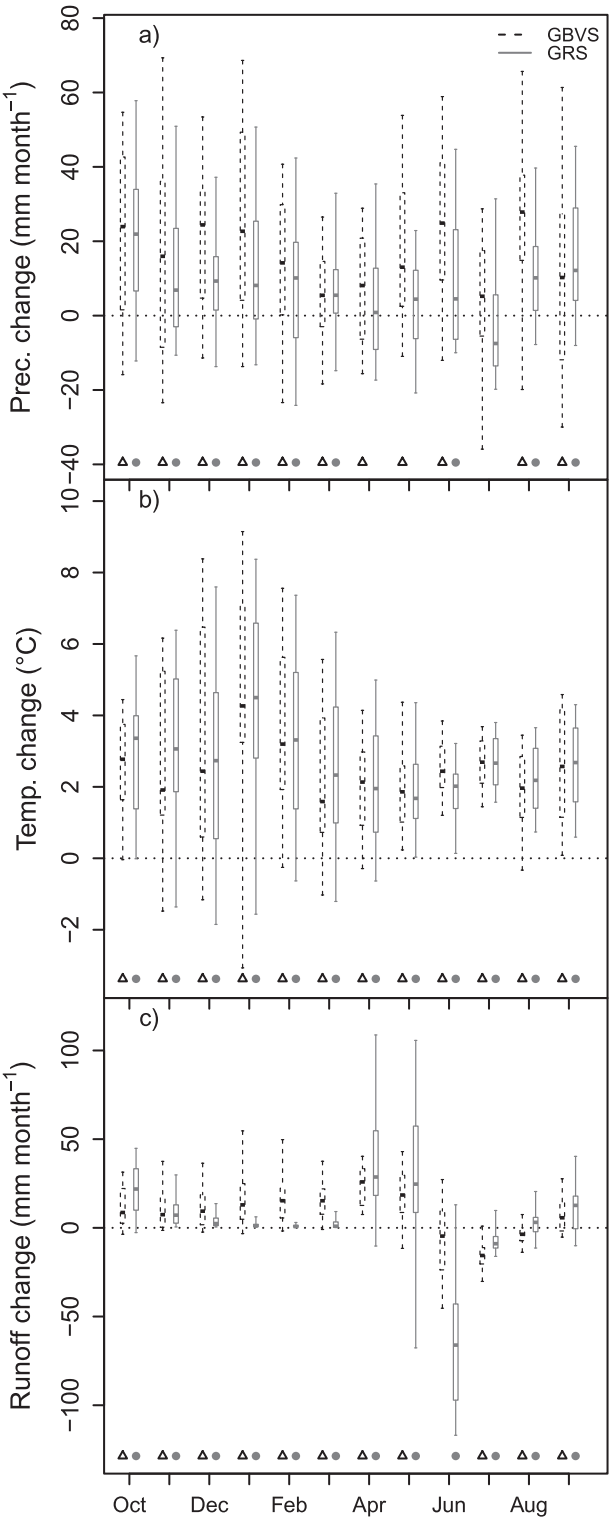

FIG. 6. As in Fig. 5, but for monthly (a) precipitation, (b) temperature, and (c) runoff changes.

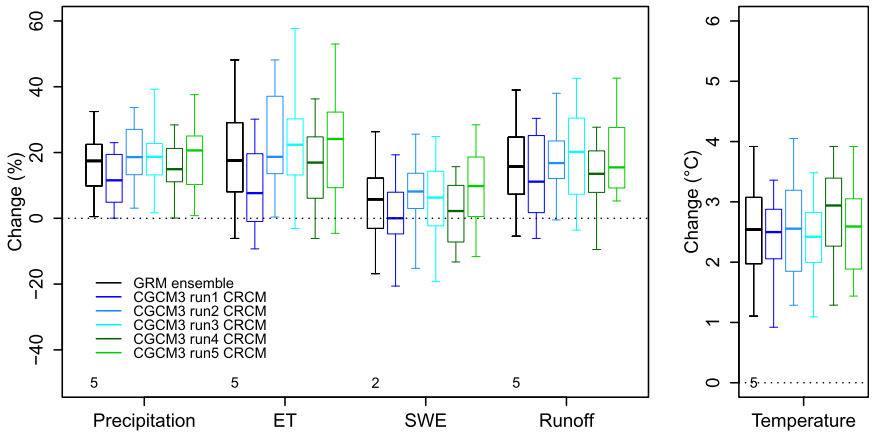

FIG. 7. Annual precipitation, evapotranspiration (ET), runoff, 1 Apr SWE changes (%), and temperature change (°C) from the GRM approach. Future changes are expressed relative to median values of the 30-yr baseline simulation of the corresponding GCM run. Each box plot illustrates the 25th, 50th, and 75th percentiles, and whiskers the 5th and 95th percentiles of the 30-yr period. The numbers at the bottom refer to the number of ensemble members (out of five) with statistically significant changes using the Student's *t* test.

(Fig. 4). The complex relationship of precipitation and temperature with snow accumulation, melt, and runoff again illustrates the problem of using the differences (between two periods) of the resultant variables for the projection of future changes when driving precipitation and temperature are biased. This also leads to an important question on the reliability of the future projections obtained from the two approaches. In summary, given that the temperature and precipitation biases are explicitly accounted for and the snow and runoff parameterization are representative (for the baseline period), the GBVS-simulated changes (i.e., increased winter and spring runoff and decreased summer runoff) can be considered physically plausible. In the case of GRS-simulated runoff, although the direction of spring (increased) and summer (decreased) runoff can be considered plausible, the magnitudes of the SWE and runoff changes do not seem plausible. Hence, the GBVS approach, for now, remains the preferred approach for projecting hydroclimatic changes. However, agreement of some of the GRS-simulated annual and monthly change signals (especially, for the driving precipitation and temperature) with GBVS shows there is potential for using RCMs for future hydroclimatic projections.

b. Comparison of GRM results

The analysis to this point has not considered the uncertainty in projections that derives from natural internal variability of the climate on multidecadal time scales. Here we consider its effects as represented by differences between the members of an ensemble of five CGCM3 simulations in the GRM experiment (see Fig. 3). The results show that the direction of change is consistent and statistically significant for all ensemble members (except for the SWE) (Fig. 7). Differences between the individual members are also generally modest; for instance, the median annual precipitation and temperature changes from the GRM ensemble members range from 12% to 21% and 2.4° to 2.9°C. Except for the relatively larger differences in the ET values (median range from 8% to 24%), variation in the range of 1 April SWE (0%–10%) and runoff (14%–17%) changes are also moderate. In all cases, variations in the medians between runs are within the interquartile range of the GRM ensemble (Fig. 7).

The results also generally depict small differences between runs in the monthly GRM simulations, both in terms of median values and ranges (Fig. 8). The changes obtained for most ensemble members are statistically significant and directions of changes, such as increased temperature and increased precipitation (for most members and most months), agree. The magnitude of changes are also similar, including greater precipitation increases in September–December and smaller increases in April–June, as well as greater temperature increases in December–February and smaller increases in March–May. The runoff changes obtained from the GRM ensemble members are also mostly similar in terms of both magnitude and timing of changes (Fig. 8c). Specifically, the peculiarities of the GRS runoff, that is, small January–March change followed by pronounced April–May increase and June decrease, are repeated for all CGCM3 runs. These results suggest that the multidecadal internal variability (as expressed by five CGCM3-driven CRCM runs) is not

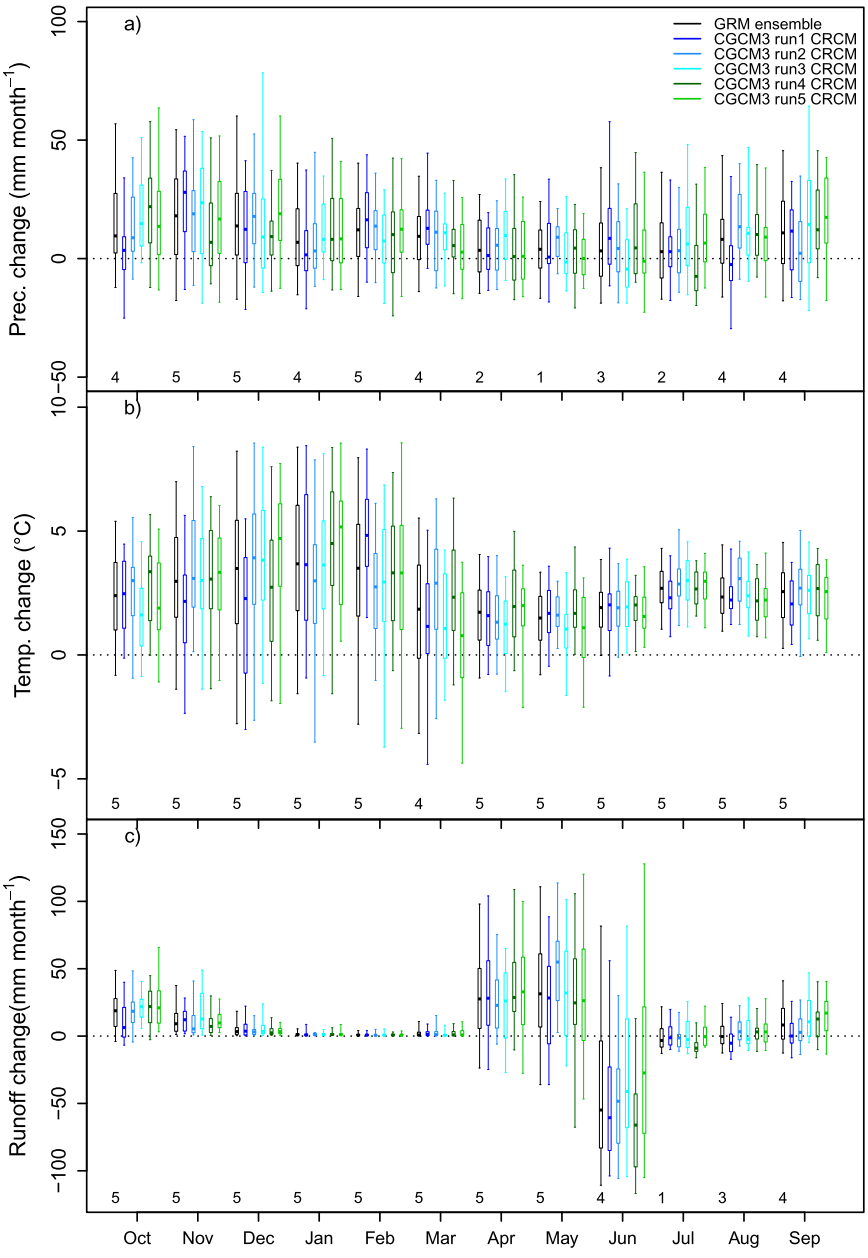

FIG. 8. As in Fig. 7, but for monthly (a) precipitation, (b) temperature, and (c) runoff changes.

a big source of uncertainty for the Peace River basin. A previous study using the five ensemble members of the CRCM (Music and Caya 2009) also found smaller differences in water budget components as a result of internal variability than those resulting from altering the land surface scheme or driving data. However, such small differences could also be due to the limited number of ensemble members, as previous studies using larger ensembles (e.g., Lucas-Picher et al. 2008; Deser et al. 2012) found considerable differences for some of the variables owing to the climate model's internal variability.

c. *Comparison of GBVM results*

We have shown, using the GBVS and GRS experiments for the historical period, that the GBVS approach provides a more plausible hydrologic response owing to explicit accounting of temperature and precipitation biases and representative snow and runoff parameterizations. Above, we have also shown that multidecadal

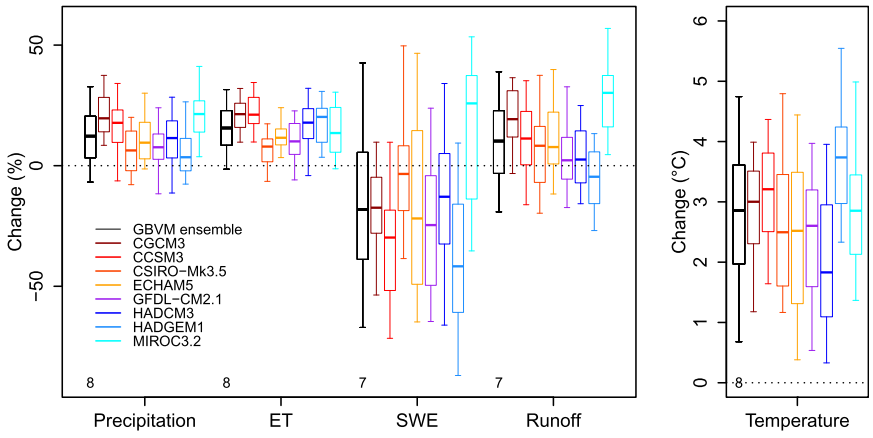

FIG. 9. Annual precipitation, evapotranspiration (ET), runoff, 1 Apr SWE changes (%), and temperature change (°C) from the GBVM approach. Future changes are expressed relative to median values of the 30-yr baseline simulation of corresponding GCM. Each box plot illustrates the 25th, 50th, and 75th percentiles, and the whiskers illustrate the 5th and 95th percentiles of the 30-yr period. The numbers at the bottom refer to the number of ensemble members (out of eight) with statistically significant changes using the Student's *t* test.

internal climate variability (as expressed by five CGCM3-driven CRCM runs) contributes only modestly to projected uncertainty in the Peace River basin. In this GBVM experiment, we consider uncertainty that is introduced by the choice of driving GCMs for the VIC model. Note that the range of annual and monthly results (Figs. 9 and 10, respectively) incorporates the uncertainties due to GCM structure (as represented by eight different GCMs) and associated internal variability. However, these figures do not depict the uncertainty inherent in the choice of downscaling method (BCSD in this case) or choice of hydrologic model (VIC in this case). Thus, overall projection uncertainty is greater than we show here, even if we do have greater confidence in the GBVS approach.

The results show noticeable differences in the annual hydroclimatic responses from different GCMs and their ensemble means (Fig. 9). The directions of precipitation, temperature, ET, 1 April SWE, and runoff changes are mostly consistent, and changes for most ensemble members are statistically significant. However, the magnitude of changes from the two approaches differs considerably. Specifically, the median annual precipitation and temperature changes from the GBVM ensemble members range from 3% to 21% and 1.8° to 3.7°C. These differences in the driving variables also lead to highly varied hydrologic responses, as illustrated by the range of median ET (7%–21%), 1 April SWE (–42% to 26%), and runoff (−4% to 30%) changes. In all cases, variations in the medians between the driving GCMs are greater than the interquartile range of the GBVM ensemble (Fig. 9).

In the case of monthly precipitation, temperature, and runoff changes, most ensemble members show statistically significant changes for most months. Besides, large differences among the different GBVM simulations can be seen in Fig. 10. For instance, some of the GCMs show greater fall–winter precipitation increases [e.g., MIROC3.2 (medres)] and summer decreases (e.g., GFDL CM2.1). The ranges (between 5th and 95th percentiles) also vary considerably. Temperature changes are also variable, with the median values showing large differences in January–March and the ranges showing large differences in November–March. These differences in the precipitation and temperature changes are reflected in the annual SWE and runoff changes (Fig. 9). Specifically, the influences of differences in seasonal change are evident, such as the greater October–January precipitation increase for MIROC3.2 (Fig. 10) resulting in greater 1 April SWE and larger runoff increase (Fig. 9). The monthly median and range of changes also show large variability, especially for May–June runoff. Such large differences in the annual and monthly hydroclimatic change signals illustrate that even with the GBVM approach, large uncertainty in the projected future hydroclimatic changes derives from the choice of GCM.

5. Summary and conclusions

The hydroclimatic response for the Peace River basin, British Columbia, was analyzed using two approaches: approach 1 (GBVS) in which statistically downscaled GCM outputs drive the VIC hydrologic model and approach 2 (GRS) in which GCM outputs are dynamically

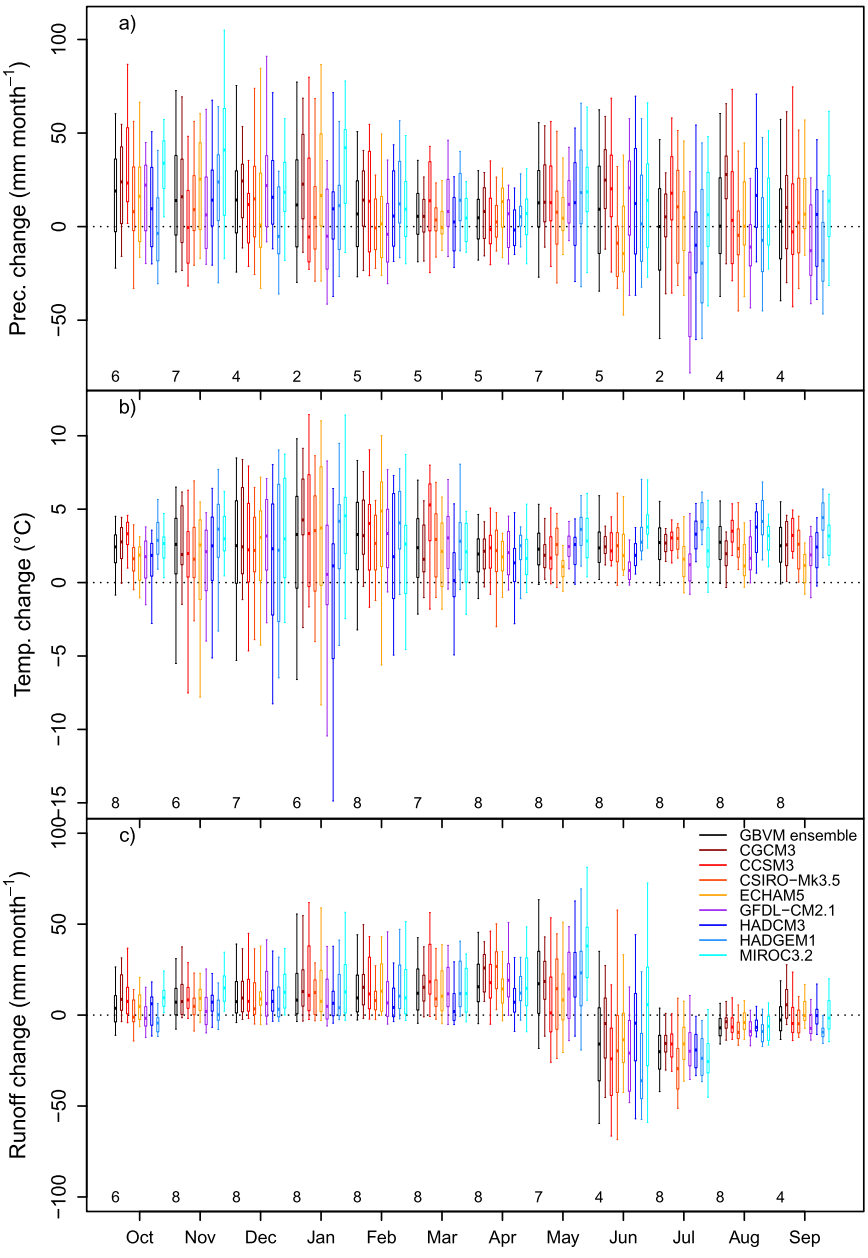

FIG. 10. As in Fig. 9, but for monthly (a) precipitation, (b) temperature, and (c) runoff changes.

downscaled with an RCM. The GBVS-simulated precipitation, temperature, and runoff agree well with observations during the baseline period thanks to bias adjustment and hydrologic model calibration. In contrast, the GRS-simulated precipitation, temperature, and runoff showed large discrepancies when compared with observations. In particular, the GRS produced an annual hydrograph with much higher and earlier peak runoff and lower winter runoff than naturalized runoff. Additionally, in spite of lower annual precipitation, the GRS approach produced higher annual runoff volume. The discrepancies (relative to observed) in the GRS-simulated precipitation and temperature can be mainly attributed to the systematic errors (biases), while discrepancies in the hydrologic response can be attributed to the propagated biases (mainly temperature bias) and model structure and parameterization.

The projected changes in the hydroclimatic variables (relative to the baseline period) from the two approaches reveal that changes in direction are mostly

consistent and changes in means are mostly statistically significant. Furthermore, the magnitude of change in the driving variables (i.e., precipitation and temperature) is similar. In the case of projected resultant hydroclimatic variables (e.g., snow water equivalent and runoff), the magnitudes of changes are considerably different, especially for the monthly results. In particular, the GRS approach projects smaller winter–spring runoff change followed by more pronounced summer runoff change, while GBVS projects appreciable winter–spring increase and smaller summer decline. These results suggest that the use of the GRS-simulated runoff and SWE changes for the projection of future changes can be problematic, when driving precipitation and temperature are biased. The assessment of the CRCM results driven by an ensemble of five CGCM3 runs (GRM) showed that these characteristics are common to all ensemble members and the variation in the medians between runs represents only a small fraction of interannual variability (range) within runs. This suggests that multidecadal internal variability (as expressed by five CGCM3-driven CRCM runs) is not a large source of uncertainty for the Peace River basin projections.

Overall, the differences between the GBVS and GRS projections emphasizes that RCM outputs should be carefully evaluated before using them for future hydroclimatic projections. For now, the approach 1 (such as the GBVS approach) remains the preferred approach for projecting basin-scale future hydrologic changes, provided that it explicitly accounts for the biases, and includes plausible snow and runoff parameterizations. However, as illustrated by an ensemble of eight GCM–VIC simulation results (GBVM), large uncertainty in the future hydroclimatic projection derives from the choice of GCM. Large differences in the annual and monthly outputs in both the driving (precipitation and temperature) and resultant (SWE and runoff) variables reinforce the need for considering the GCM uncertainties in projecting future hydroclimatic changes.

Uncertainties in driving GCMs will also affect the RCM-simulated results, which should be a focus for future research, for example, by employing multiple RCMs driven by multiple GCMs from the NARCCAP projects (Mearns et al. 2009). Similarity of some of the GRS-simulated changes with the GBVS (especially annual) shows that there is potential for using RCMs for hydroclimatic projections. Some of the issues related to the RCMs, such as the coarser spatial resolution, can be expected to be addressed in future generations of RCMs (e.g., CORDEX) (Giorgi et al. 2009). Further enhancements such as reduction of biases and better representation of the land surface parameterization can also be expected in the future versions of regional climate models. With such enhancements, the RCMs can be expected to provide improved representations of basin-scale hydroclimatology.

Acknowledgments. We acknowledge the financial support of BC Hydro for this study. We would like to acknowledge Biljana Music, Marco Braun, and Daniel Caya (all Ouranos) for providing CRCM run results for this study. Dave Rodenhuis (PCIC) is acknowledged for the CRCM result analyses in the previous study (Rodenhuis et al. 2011), which form the basis for this study. The authors are thankful to Anne Berland and Hailey Eckstrand for data processing for this study. We would also like to thank three anonymous reviewers for their comments, which led to an improved version of the manuscript.

REFERENCES

Allen, D. M., A. J. Cannon, M. W. Toews, and J. Scibek, 2010: Variability in simulated recharge using different GCMs. *Water Resour. Res.,* **46,** W00F03, doi:10.1029/2009WR008932.

Bartlett, P. A., M. D. MacKay, and D. L. Verseghy, 2006: Modified snow algorithms in the Canadian land surface scheme: Model runs and sensitivity analysis at three boreal forest stands. *Atmos.–Ocean,* **44,** 207–222, doi:10.3137/ao.440301.

Bennett, K. E., A. T. Werner, and M. Schnorbus, 2012: Uncertainties in hydrologic and climate change impact analyses in headwater basins of British Columbia. *J. Climate,* **25,** 5711–5730, doi:10.1175/JCLI-D-11-00417.1.

Bürger, G., T. Q. Murdock, A. T. Werner, S. R. Sobie, and A. J. Cannon, 2012: Downscaling extremes—An intercomparison of multiple statistical methods for present climate. *J. Climate,* **25,** 4366–4388, doi:10.1175/JCLI-D-11-00408.1.

Collins, M., S. Tett, and C. Cooper, 2001: The internal climate variability of HadCM3, a version of the Hadley Centre coupled model without flux adjustments. *Climate Dyn.,* **17,** 61–81, doi:10.1007/s003820000094.

Collins, W., and Coauthors, 2006: The Community Climate System Model version 3 (CCSM3). *J. Climate,* **19,** 2122–2143, doi:10.1175/JCLI3761.1.

Davison, B., S. Pohl, P. Domes, P. Marsh, A. Pietroniro, and M. MacKay, 2006: Characterizing snowmelt variability in a land-surface-hydrologic model. *Atmos.–Ocean,* **44,** 271–287, doi:10.3137/ao.440305.

Delworth, T., and Coauthors, 2006: GFDL's CM2 global coupled climate models. Part I: Formulation and simulation characteristics. *J. Climate,* **19,** 643–674, doi:10.1175/JCLI3629.1.

Demarchi, D. A., cited 2011: The British Columbia Ecoregion Classification, third edition. Ministry of Environment, Victoria, British Columbia, Canada. [Available online at http://www.env.gov.bc.ca/ecology/ecoregions/intro.html.]

Deser, C., A. Phillips, V. Bourdette, and H. Teng, 2012: Uncertainty in climate change projections: The role of internal variability. *Climate Dyn.,* **38,** 527–546, doi:10.1007/s00382-010-0977-x.

Dornes, P. F., J. W. Pomeroy, A. Pietroniro, and D. L. Verseghy, 2008: Effects of spatial aggregation of initial conditions and forcing data on modeling snowmelt using a land surface scheme. *J. Hydrometeor.,* **9,** 789–803, doi:10.1175/2007JHM958.1.

Elsner, M. M., and Coauthors, 2010: Implications of 21st century climate change for the hydrology of Washington State. *Climatic Change,* **102,** 225–260, doi:10.1007/s10584-010-9855-0.

Gao, Y., J. A. Vano, C. Zhu, and D. P. Lettenmaier, 2011: Evaluating climate change over the Colorado River basin using regional climate models. *J. Geophys. Res.,* **116,** D13104, doi:10.1029/2010JD015278.

Giorgi, F., C. Jones, and G. R. Asrar, 2009: Addressing climate information needs at the regional level: The CORDEX framework. *WMO Bull.,* **58,** 175–183.

Global Soil Data Task, 2000: *Global Soil Data Products CD-ROM (IGBP-DIS).* International Geosphere–Biosphere Programme, Data and Information System, CD-ROM.

Hidalgo, H. G., and Coauthors, 2009: Detection and attribution of streamflow timing changes to climate change in the western United States. *J. Climate,* **22,** 3838–3855, doi:10.1175/2009JCLI2470.1.

Jarvis, A., H. I. Reuter, A. Nelson, and E. Guevara, cited 2008: Hole-filled seamless SRTM data V4 583. International Centre for Tropical Agriculture (CIAT). [Available online at: http://srtm.csi.cgiar.org.]

K-1 Model Developers, 2004: K-1 coupled GCM (MIROC) description. H. Hasumi and S. Emori, Eds., K-1 Tech. Rep. 1, Center for Climate System Research, University of Tokyo. [Available online at http://ccsr.aori.u-tokyo.ac.jp/~hasumi/miroc_description.pdf.]

Kalnay, E., and Coauthors, 1996: The NCEP/NCAR 40-Year Reanalysis Project. *Bull. Amer. Meteor. Soc.,* **77,** 437–471, doi:10.1175/1520-0477(1996)077<0437:TNYRP>2.0.CO;2.

Kay, A. L., H. N. Davies, V. A. Bell, and R. G. Jones, 2008: Comparison of uncertainty sources for climate change impacts: Flood frequency in England. *Climatic Change,* **92,** 41–63, doi:10.1007/s10584-008-9471-4.

Kendon, E. J., R. G. Jones, E. Kjellström, and J. M. Murphy, 2010: Using and designing GCM–RCM ensemble regional climate projections. *J. Climate,* **23,** 6485–6503, doi:10.1175/2010JCLI3502.1.

Langlois, A., A. Royer, E. Fillol, A. Frigon, and R. Laprise, 2004: Evaluation of the snow cover variation in the Canadian Regional Climate Model over eastern Canada using passive microwave satellite data. *Hydrol. Processes,* **18,** 1127–1138, doi:10.1002/hyp.5514.

Liang, X., D. P. Lettenmaier, E. F. Wood, and S. J. Burges, 1994: A simple hydrologically based model of land-surface water and energy fluxes for general-circulation models. *J. Geophys. Res.,* **99** (D7), 14 415–14 428, doi:10.1029/94JD00483.

——, E. F. Wood, and D. P. Lettenmaier, 1996: Surface soil moisture parameterization of the VIC-2L model: Evaluation and modification. *Global Planet. Change,* **13,** 195–206, doi:10.1016/0921-8181(95)00046-1.

——, Z. Xie, and M. Huang, 2003: A new parameterization for surface and groundwater interactions and its impact on water budgets with the variable infiltration capacity (VIC) land surface model. *J. Geophys. Res.,* **108,** 8613, doi:10.1029/2002JD003090.

Lucas-Picher, P., D. Caya, R. de Elia, and R. Laprise, 2008: Investigation of regional climate models' internal variability with a ten-member ensemble of 10-year simulations over a large domain. *Climate Dyn.,* **31,** 927–940, doi:10.1007/s00382-008-0384-8.

Maidment, D. R., Ed., 1993: *Handbook of Hydrology*. McGraw-Hill, 1424 pp.

Martin, G., M. Ringer, V. Pope, A. Jones, C. Dearden, and T. Hinton, 2006: The physical properties of the atmosphere in the new Hadley Centre Global Environmental Model (HadGEM1). Part I: Model description and global climatology. *J. Climate,* **19,** 1274–1301, doi:10.1175/JCLI3636.1.

Maurer, E. P., and H. G. Hidalgo, 2008: Utility of daily vs. monthly large-scale climate data: An intercomparison of two statistical downscaling methods. *Hydrol. Earth Syst. Sci.,* **12,** 551–563, doi:10.5194/hess-12-551-2008.

Mearns, L. O., W. J. Gutowski, R. Jones, L.-Y. Leung, S. McGinnis, A. M. B. Nunes, and Y. Qian, 2009: A regional climate change assessment program for North America. *Eos, Trans. Amer. Geophys. Union,* **90,** 311–312, doi:10.1029/2009EO360002.

Meehl, G. A., C. Covey, K. E. Taylor, T. Delworth, R. J. Stouffer, M. Latif, B. McAvaney, and J. F. B. Mitchell, 2007: The WCRP CMIP3 multimodel dataset: A new era in climate change research. *Bull. Amer. Meteor. Soc.,* **88,** 1383–1394, doi:10.1175/BAMS-88-9-1383.

Merritt, W. S., Y. Alila, M. Barton, B. Taylor, S. Cohen, and D. Neilsen, 2006: Hydrologic response to scenarios of climate change in sub watersheds of the Okanagan basin, British Columbia. *J. Hydrol.,* **326,** 79–108, doi:10.1016/j.jhydrol.2005.10.025.

Muerth, M. J., and Coauthors, 2013: On the need for bias correction in regional climate scenarios to assess climate change impacts on river runoff. *Hydrol. Earth Syst. Sci.,* **17,** 1189–1204, doi:10.5194/hess-17-1189-2013.

Music, B., and D. Caya, 2007: Evaluation of the hydrological cycle over the Mississippi River basin as simulated by the Canadian regional climate model (CRCM). *J. Hydrometeor.,* **8,** 969–988, doi:10.1175/JHM627.1.

——, and ——, 2009: Investigation of the sensitivity of water cycle components simulated by the Canadian Regional Climate Model to the land surface parameterization, the lateral boundary data, and the internal variability. *J. Hydrometeor.,* **10,** 3–21, doi:10.1175/2008JHM979.1.

——, ——, A. Frigon, M. Slivitzky, A. Musy, R. Roy, and D. Rodenhuis, 2012: Canadian Regional Climate Model (CRCM) as a tool for assessing hydrological impacts of climate change at the watershed scale. *Climatic Change,* A. Berger et al., Eds., Springer-Verlag, 157–165, doi:10.1007/978-3-7091-0973-1_12.

Najafi, M. R., H. Moradkhani, and I. W. Jung, 2011: Assessing the uncertainties of hydrologic model selection in climate change impact studies. *Hydrol. Processes,* **25,** 2814–2826, doi:10.1002/hyp.8043.

Plummer, D. A., and Coauthors, 2006: Climate and climate change over North America as simulated by the Canadian RCM. *J. Climate,* **19,** 3112–3132, doi:10.1175/JCLI3769.1.

Poitras, V., L. Sushama, F. Seglenieks, M. N. Khaliq, and E. Soulis, 2011: Projected changes to streamflow characteristics over western Canada as simulated by the Canadian RCM. *J. Hydrometeor.,* **12,** 1395–1413, doi:10.1175/JHM-D-10-05002.1.

Prudhomme, C., and H. Davies, 2008a: Assessing uncertainties in climate change impact analyses on the river flow regimes in the UK. Part 1: Baseline climate. *Climatic Change,* **93,** 177–195, doi:10.1007/s10584-008-9464-3.

——, and ——, 2008b: Assessing uncertainties in climate change impact analyses on the river flow regimes in the UK. Part 2: Future climate. *Climatic Change,* **93,** 197–222, doi:10.1007/s10584-008-9461-6.

Rauscher, S. A., J. S. Pal, N. S. Diffenbaugh, and M. M. Benedetti, 2008: Future changes in snowmelt-driven runoff timing over the western US. *Geophys. Res. Lett.,* **35,** L16703, doi:10.1029/2008GL034424.

Rivington, M., D. Miller, K. B. Matthews, G. Russell, G. Bellocchi, and K. Buchan, 2008: Evaluating regional climate model

estimates against site-specific observed data in the UK. *Climatic Change,* **88,** 157–185, doi:10.1007/s10584-007-9382-9.

Rodenhuis, D., B. Music, M. Braun, and D. Caya, 2011: Climate diagnostics of future water resources in BC watersheds. Regional Climate Modelling Diagnostics Project Final Rep., Pacific Climate Impacts Consortium, University of Victoria, Victoria, BC, Canada, 74 pp. [Available online at http://www.pacificclimate.org/sites/default/files/publications/Rodenhuis.RCMDiagnostics.FinalReport.Apr2011.pdf.]

Roeckner, E., and Coauthors, 2006: Sensitivity of simulated climate to horizontal and vertical resolution in the ECHAM5 atmosphere model. *J. Climate,* **19,** 3771–3791, doi:10.1175/JCLI3824.1.

Rotstayn, L., M. Collier, M. Dix, Y. Feng, H. Gordon, S. O'Farrell, I. Smith, and J. Syktus, 2010: Improved simulation of Australian climate and ENSO-related rainfall variability in a global climate model with an interactive aerosol treatment. *Int. J. Climatol.,* **30,** 1067–1088.

Salathé, E. P., L. R. Leung, Y. Qian, and Y. Zhang, 2010: Regional climate model projections for the State of Washington. *Climatic Change,* **102,** 51–75, doi:10.1007/s10584-010-9849-y.

Schnorbus, M., K. Bennett, and A. Werner, 2010: Quantifying the water resource impacts of mountain pine beetle and associated salvage harvest operations across a range of watershed scales: Hydrologic modeling of the Fraser River basin. Information Rep. BC-X-423, Canadian Forest Service Pacific Forestry Centre, Victoria, BC, Canada, 63 pp. [Available online at http://cfs.nrcan.gc.ca/pubwarehouse/pdfs/31207.pdf.]

——, ——, ——, and A. J. Berland, 2011: Hydrologic impacts of climate change in the Peace, Campbell and Columbia Watersheds, British Columbia, Canada. Hydrologic Modelling Project Final Rep. (Part II), Pacific Climate Impacts Consortium, University of Victoria, Victoria, BC, Canada, 157 pp. [Available online at http://www.pacificclimate.org/sites/default/files/publications/Schnorbus.HydroModelling.FinalReport2.Apr2011.pdf.]

——, A. T. Werner, and K. E. Bennett, 2014: Impacts of climate change in three hydrologic regimes in British Columbia, Canada. *Hydrol. Processes,* **28,** 1170–1189, doi:10.1002/hyp.9661.

Scinocca, J. F., N. A. McFarlane, M. Lazare, J. Li, and D. Plummer, 2008: Technical note: The CCCma third generation AGCM and its extension into the middle atmosphere. *Atmos. Chem. Phys.,* **8,** 7055–7074, doi:10.5194/acp-8-7055-2008.

Shrestha, R. R., A. J. Berland, M. A. Schnorbus, and A. T. Werner, 2011: Climate Change Impacts on Hydro-Climatic Regimes in the Peace and Columbia Watersheds, British Columbia, Canada. Synthesis Project Final Rep., Pacific Climate Impacts Consortium, University of Victoria, Victoria, BC, Canada, 37 pp. [Available online at http://www.pacificclimate.org/sites/default/files/publications/Shrestha.Synthesis.FinalReport.Apr2011.pdf.]

——, Y. B. Dibike, and T. D. Prowse, 2012a: Modelling of climate-induced hydrologic changes in the Lake Winnipeg watershed. *J. Great Lakes Res.,* **38** (3), 83–94, doi:10.1016/j.jglr.2011.02.004.

——, M. A. Schnorbus, A. T. Werner, and A. J. Berland, 2012b: Modelling spatial and temporal variability of hydrologic impacts of climate change in the Fraser River basin, British Columbia, Canada. *Hydrol. Processes,* **26,** 1840–1860, doi:10.1002/hyp.9283.

Stahl, K., R. D. Moore, J. M. Shea, D. Hutchinson, and A. J. Cannon, 2008: Coupled modelling of glacier and streamflow response to future climate scenarios. *Water Resour. Res.,* **44,** W02422, doi:10.1029/2007WR005956.

Sulis, M., C. Paniconi, C. Rivard, R. Harvey, and D. Chaumont, 2011: Assessment of climate change impacts at the catchment scale with a detailed hydrological model of surface-subsurface interactions and comparison with a land surface model. *Water Resour. Res.,* **47,** W01513, doi:10.1029/2010WR009167.

Sushama, L., R. Laprise, D. Caya, A. Frigon, and M. Slivitzky, 2006: Canadian RCM projected climate-change signal and its sensitivity to model errors. *Int. J. Climatol.,* **26,** 2141–2159, doi:10.1002/joc.1362.

Teutschbein, C., and J. Seibert, 2012: Bias correction of regional climate model simulations for hydrological climate-change impact studies: Review and evaluation of different methods. *J. Hydrol.,* **456–457,** 12–29, doi:10.1016/j.jhydrol.2012.05.052.

Todini, I., 1996: The ARNO rainfall–runoff model. *J. Hydrol.,* **175,** 339–382, doi:10.1016/S0022-1694(96)80016-3.

Vano, J. A., N. Voisin, L. Cuo, A. F. Hamlet, M. M. Elsner, R. N. Palmer, A. Polebitski, and D. P. Lettenmaier, 2010: Climate change impacts on water management in the Puget Sound region, Washington State, USA. *Climatic Change,* **102,** 261–286, doi:10.1007/s10584-010-9846-1.

Verseghy, D. L., 1991: Class—A Canadian land surface scheme for GCMS. I. Soil model. *Int. J. Climatol.,* **11,** 111–133, doi:10.1002/joc.3370110202.

——, 2000: The Canadian land surface scheme (CLASS): Its history and future. *Atmos.–Ocean,* **38,** 1–13, doi:10.1080/07055900.2000.9649637.

——, N. A. McFarlane, and M. Lazare, 1993: Class—A Canadian land surface scheme for GCMS, II. Vegetation model and coupled runs. *Int. J. Climatol.,* **13,** 347–370, doi:10.1002/joc.3370130402.

von Storch, H., and F. Zwiers, 1999: *Statistical Analysis in Climate Research.* Cambridge University Press, 484 pp.

——, and ——, 2013: Testing ensembles of climate change scenarios for ''statistical significance.'' *Climatic Change,* **117,** 1–9, doi:10.1007/s10584-012-0551-0.

Werner, A. T., 2011: BCSD downscaled transient climate projections for eight select GCMs over British Columbia, Canada. Hydrologic Modelling Project Final Rep. (Part I), Pacific Climate Impacts Consortium, University of Victoria, Victoria, BC, Canada, 63 pp. [Available online at http://www.pacificclimate.org/sites/default/files/publications/Werner.HydroModelling.FinalReport1.Apr2011.pdf.]

Wilby, R. L., L. E. Hay, W. J. Gutowski Jr., R. W. Arritt, E. S. Takle, Z. Pan, G. H. Leavesley, and M. P. Clark, 2000: Hydrological responses to dynamically and statistically downscaled climate model output. *Geophys. Res. Lett.,* **27,** 1199–1202, doi:10.1029/1999GL006078.

Winter, J. M., and E. A. B. Eltahir, 2011a: Modeling the hydroclimatology of the midwestern United States. Part 1: Current climate. *Climate Dyn.,* **38,** 573–593, doi:10.1007/s00382-011-1182-2.

——, and ——, 2011b: Modeling the hydroclimatology of the midwestern United States. Part 2: Future climate. *Climate Dyn.,* **38,** 595–611, doi:10.1007/s00382-011-1183-1.

Wood, A. W., E. P. Maurer, A. Kumar, and D. P. Lettenmaier, 2002: Long-range experimental hydrologic forecasting for the eastern United States. *J. Geophys. Res.,* **107,** 4429, doi:10.1029/2001JD000659.

——, L. Leung, V. Sridhar, and D. P. Lettenmaier, 2004: Hydrologic implications of dynamical and statistical approaches to downscaling climate model outputs. *Climatic Change,* **62,** 189–216, doi:10.1023/B:CLIM.0000013685.99609.9e.

Wulder, M., J. Dechka, M. Gillis, J. Luther, R. Hall, and A. Beaudoin, 2003: Operational mapping of the land cover of the forested area of Canada with Landsat data: EOSD land cover program. *For. Chron.,* **79,** 1075–1083. [Available online at http://cfs.nrcan.gc.ca/pubwarehouse/pdfs/23696.pdf.]